Int. J. Electrochem. Sci., 10 **(2015)** 3600 - 3612

International Journal of ELECTROCHEMICAL SCIENCE
www.electrochemsci.org

Structure Modification to Tune the Electronic and Charge Transport Properties of Solar Cell Materials: Quantum Chemical Study

Ahmad Irfan[1,*], *Shabbir Muhammad*[2], *Abdullah G. Al-Sehemi*[1,3,4], *Mohammad Sultan Al-Assiri*[5,6], *Abul Kalam*[1]

[1] Department of Chemistry, Faculty of Science, King Khalid University, Abha 61413, P.O. Box 9004, Saudi Arabia
[2] Department of Physics, Faculty of Science, King Khalid University, Abha 61413, P.O. Box 9004, Saudi Arabia
[3] Unit of Science and technology, Faculty of Science, King Khalid University, Abha 61413, P.O. Box 9004, Saudi Arabia
[4] Research Center for Advanced Materials Research, King Khalid University, Abha 61413, P.O. Box 9004, Saudi Arabia.
[5] Department of Physics, Faculty of Sciences and Arts, Najran University, P.O. Box 1988, Najran 11001, Saudi Arabia
[6] Promising Centre for Sensors and Electronic Devices (PCSED), Najran University, P.O. Box 1988, Najran 11001, Saudi Arabia
[*]E-mail: irfaahmad@gmail.com

Received: 20 November 2014 / *Accepted:* 11 January 2015 / *Published:* 24 February 2015

The ground states geometries of naphtho[2,3-b]thiophene derivatives have been optimized by using density functional theory (DFT) at B3LYP/6-31G** level of theory. The excitation energies have been computed by using time dependent DFT. The investigated dyes have been investigated with respect to dye-sensitized solar cells (DSSCs) and hetero-junction hybrid solar cells. The electron injection (ΔG_r^{inject}), electron coupling constants ($|V_{RP}|$) and light harvesting efficiencies (LHE) of studied compounds have been discussed with esteem to DSSCs. The ΔG_r^{inject} and $|V_{RP}|$ of new designed derivatives showed that these materials would be efficient DSSC materials. The electron affinities, reorganization energies, diagonal band gaps, and energy level offsets have been studied to shed light on the electron transfer behavior of studied materials with respect to hetero-junction hybrid solar cells. The higher electron affinities of **2**, **4** and **6** revealed that the electron transport toward cathode in hetero-junction solar cells would be superior ultimately improve the open circuit photovoltage (V_{oc}). The higher diagonal band gap for **2**, **4** and **6** compared to their counterparts (**1**, **3** and **5**) showed that these dyes might have higher short-circuit current density (J_{sc}) and fill factor (FF). The hole and electron reorganization energies showed that these materials would be efficient charge transporters.

Keywords: Solar cells; Naphtho[2,3-b]thiophene derivatives; 2-{4-[2-(4-Nitrobenzylidene)hydrazino)]phenyl}ethylene 1,1,2-tricarbonitrile; Density functional Theory; Charge transport, diagonal band gap; Electronic structure

1. INTRODUCTION

The organic materials, visible light sensing and absorbing sensitizers and sensors are getting increasing attention as possible substitutes to traditional inorganic counterparts [1-3]. The Ru complexes showed the efficiency up to 10% as photosensitizers but these have health and environmental issues [4]. The organic materials are being used in photovoltaic devices which have low cost, environmental friendly and easy to fabricate [5]. The dye-sensitized solar cells (DSSCs) [6, 7] and hetero-junction hybrid solar cells with different nanoparticles such as TiO_x [8], ZnO [9], CdSe [10] [11], CdS [12], PbS [13], $CuInS_2$ [14] have been investigated in recent years. The organic/inorganic (organic/Si) hybrid solar cells gained much attention recently [15-20]. In organic-inorganic hybrid solar cells generally organic and inorganic parts have been combined with the aim to gain the advantages coupled with both material groups [21, 22].

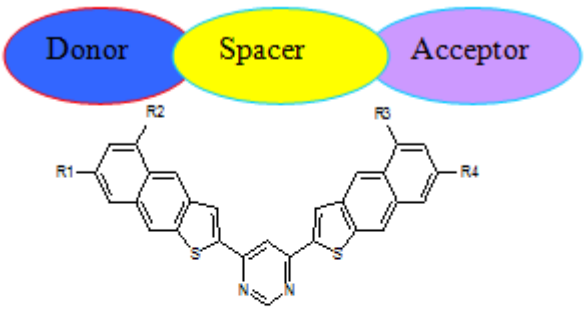

1; R1, R2 = CH_3; R3, R4 = COOH
2; R1, R2 = CH_3; R3, R4 = NO_2
3; R1, R2 = OCH_3; R3, R4 = COOH
4; R1, R2 = OCH_3; R3, R4 = NO_2
5; R1, R2 = OH; R3, R4 = COOH
6; R1, R2 = OH; R3, R4 = NO_2

Figure 1. The donor-bridge-acceptor systems investigated in present study.

The basic structure of organic sensitizers is made of a donor (D), a bridge (B, π spacer), and an acceptor (A) moieties (D-π-A) to improve the efficiency of the UV/Vis photoinduced intra-molecular charge transfer (ICT). Generally, the critical factors that influence the sensitization are (i) a huge light harvesting ability of the dye is critical to get a significant photocurrent response; (ii) the good conjugation across the donor and acceptor group establishes the large CT character of the electronic transition; (iii) the electronic coupling strength is leading property for an efficient electron injection from the dye onto the semiconductor surface [23]. Previously, it has been found that by sandwiching

the electron deficient moiety between electrons rich ones enhanced the ICT [24], charge transport [25] and tuned the electrochemical/spectroscopic properties [26]. The oligoacenes (e.g. naphthalene to hexacene) are being used as molecular backbones [27] in organic semiconductors due to their proficient electronic properties [28]. We have designed donor-bridge-acceptor (D-π-A) naphtho[2,3-b]thiophene derivatives by incorporating the electron-rich and electron-deficient units, Fig. 1 which would enhance the ICT, tune the electro-optical and charge transport properties.

In the present study we have substituted the CH_3, OH and OCH_3 at one end to augment the electron-donor ability. The ICT process plays a vital role in achieving higher efficiency which has been improved by introducing strong electron deactivating anchoring groups COOH and NO_2. We shed light on ICT and energy transfer (ET) of the newly designed derivatives. We studied the effect of donor groups as it is expected that strong electron donor groups at one end and acceptor moiety at opposite side would tune the ICT through bridge, ultimately it would enhance the electron injection and electron coupling constant. It is anticipated that improved ICT would also improve the harvesting ability of sensitizers. The ICT process also plays a crucial role in achieving higher efficiency. This investigation aims helping to design efficient organic dyes in future that deliver qualitatively good descriptions of the electron injection of D-π-A sensitizers. The aim is also to design such derivatives which would be good materials as hetero-junction solar cells.

The time-dependent density functional theory (TDDFT) has been used for the excitation energy calculations. The quantum chemical calculations have been performed to gain insight into electronic and charge transfer properties. We have also discussed the structure-property relationship. On the basis of electron injection, electronic coupling constants, light harvesting efficiencies, reorganization energies, electron affinities and energy level offset the nature of materials has been explained. The technical finding of the manuscript is interesting, and it potentially has applications for motivating experimentalists in pursuing the various donor and acceptor substitutions with various molecules. The paper is structured as follows: Section 2 deals about the methodology adopted; Section 3 discusses the charge transfer properties of studied systems as sensitizers and hetero-junction solar cells; the last section focuses on the major conclusions.

2. COMPUTATIONAL DETAILS

The ground state geometries have been optimized at ground state by using density functional theory (DFT) [29-51]. The computations of the excitation energies for dye sensitizers were performed using TDDFT with Gaussian09 package [52]. We have applied B3LYP [53-55] with 6-31G** basis set [56]. The TDDFT was used to investigate the light harvesting efficiency and excitation energies of sensitizers which have been proved an efficient approach [57, 58].

The description of the electron transfer from a dye to a semiconductor, the rate of the charge transfer process can be derived from the general classical Marcus theory [59] [60-62] [63],

$$k_{inject.} = |V_{RP}|^2/h\,(\pi/\lambda k_B T)^{1/2} \exp[-(\Delta G^{inject.} + \lambda)^2/4\lambda k_B T] \quad (1)$$

In eq. (1), $k_{inject.}$ is the rate constant (in S^{-1}) of the electron injection from dye to TiO_2, k_{BT} is the Boltzmann thermal energy, h the Planck constant, $-\Delta G^{inject.}$ the free energy of injection and λ is the

reorganization energy of the system, $|V_{RP}|$ is the coupling constant between the reagent and the product potential curves. Eq (1) revealed that larger $|V_{RP}|$ leads to higher rate constant which would result better sensitizer. The value of $|V_{RP}|$ defines the adiabatic or non-adiabatic character of the electron transfer. The use of the Generalized Mulliken-Hush formalism (GMH) allows evaluating $|V_{RP}|$ for a photoinduced charge transfer [60, 61]. The Hsu et al. explained that $|V_{RP}|$ can be evaluated as [61].

$$|V_{RP}| = \Delta E_{RP}/2 \quad (2)$$

The injection driving force can be formally expressed within Koopmans approximation as

$$\Delta E_{RP} = [\, E^{dye}_{LUMO} + 2\, E^{dye}_{HOMO} \,] - [\, E^{dye}_{LUMO} + E^{dye}_{HOMO} + E^{TiO2}_{CB} \,] \quad (3)$$

where E^{TiO2}_{CB} is the conduction band edge. It is often difficult to accurately determine E^{TiO2}_{CB} because it is highly sensitive to the conditions, e.g. the pH of the solution. Thus we used experimental value corresponding to conditions where the semiconductor is in contact with aqueous redox electrolytes of fixed pH 7.0, i.e., E^{TiO2}_{CB} = -4.0 eV [64-66].

More quantitatively for a closed-shell system E^{dye}_{LUMO} corresponds to the reduction potential of the dye (E^{dye}_{RED}), whereas the HOMO energy is related to the potential of first oxidation (i. e., - E^{dye}_{HOMO} = E^{dye}_{OX}). As a result eq. (3) becomes,

$$\Delta E_{RP} = [\, E^{dye}_{HOMO} - E^{dye}_{OX} \,] = - [\, E^{dye}_{OX} + E^{TiO2}_{CB} \,] \quad (4)$$

The eq (4) can be rewritten as

$$\Delta E_{RP} = E^{dye}_{0-0} - [2\, E^{dye}_{OX} + E^{dye}_{RED} + E^{TiO2}_{CB} \,] \quad (5)$$

We propose to establish a reliable theoretical scheme to evaluate the dye's excited state oxidation potential and quantify the electron injection onto a titanium dioxide (TiO_2) surface. The free energy change (in electron volts, eV) for the electron injection can be expressed as [65].

$$\Delta G^{inject} = E^{dye^*}_{OX} - E^{TiO2}_{CB} \quad (6)$$

where $E^{dye^*}_{OX}$ is the oxidation potential of the dye in the excited state and E^{TiO2}_{CB} is the reduction potential of the semiconductor conduction band. Two models can be used for the evaluation of $E^{dye^*}_{OX}$ [67, 68]. The first implies that the electron injection occurs from the unrelaxed excited state. For this reaction path, the excited state oxidation potential can be extracted from the redox potential of the ground state, E^{dye}_{OX} and the vertical transition energy corresponding to the photoinduced ICT,

$$E^{dye^*}_{OX} = E^{dye}_{OX} - \lambda^{ICT}_{max} \quad (7)$$

where λ^{ICT}_{max} is the energy of the ICT. Note that this relation is only valid if the entropy change during the light absorption process can be neglected. For the second model, one assumes that electron injection occurs after relaxation. Given this condition, $E^{dye^*}_{OX}$ is expressed as [68]:

$$E^{dye^*}_{OX} = E^{dye}_{OX} - E^{dye}_{0-0} \quad (8)$$

where E^{dye}_{0-0} is the 0-0 transition energy between the ground state and the excited state. To estimate the 0-0 "absorption" line, we need both the S_0 (singlet ground state) and the S_1 (first singlet excited state) equilibrium geometries, Q_{S0} and Q_{S1}, respectively. Though electron injection from

unrelaxed excited states has been observed in TiO_2 [69] and SnO_2 [70], the relative contribution of an ultrafast injection path is not clear, and the most experimental groups assume that the electron injection dominantly occurs after relaxation. Preat et al. concluded that the absolute difference between the relaxed and unrelaxed $\Delta G_{\text{inject.}}$ is constant, and is of the same order of magnitude than the E_{OX}^{dye} and E_{OX}^{dye*} mean average error (MAE) [71]. The ΔG^{inject} and E_{OX}^{dye*} have been evaluated using Eqs. (6) and (7).

The LHE of the dye has to be as high as possible to maximize the photocurrent response. The LHE can be expressed as [72]:

$$\text{LHE} = 1 - 10^{-\text{A}} = 1 - 10^{-f} \tag{9}$$

where A (f) is the absorption (oscillator strength) of the dye associated to the $\lambda_{\max}^{ICT}$. The oscillator strength is directly derived from the TDDFT calculations as follow:

$$f = \frac{2}{3}\lambda_{\max}^{\text{ICT}} |\vec{\mu}_{0-\text{ICT}}|^2 \tag{10}$$

where $\mu_{0-\text{ICT}}$ is the dipolar transition moment associated to the electronic excitation. In order to maximize f, both $\lambda_{\max}^{ICT}$ and $\mu_{0-\text{ICT}}$ must be large [73, 74].

The efficiency (η) of solar cells can be determined by using the following equation

$$\eta = FF\frac{V_{oc}J_{sc}}{P_{in}}$$

where J_{sc} is the short-circuit current density, V_{oc} is the opencircuit photovoltage, FF is the fill factor, and $P_{\text{inc.}}$ is the intensity of the incident light. The J_{sc} can be evaluated as $J_{sc} = \int_{\lambda} LHE(\lambda)\phi_{injection}\eta_{collection}d\lambda$

where $\eta_{collection}$ is the charge collection efficiency which is constant. From above equation, we can find that J_{sc} is directly linked with the LHE and $\phi_{injection}$ is electron injection efficiency which is related to ΔG^{inject}. It is revealing that higher LHE and ΔG^{inject} would lead efficient devices [75].

$$J_{sc} = \int_{\lambda} LHE(\lambda)\phi_{injection}\eta_{collection}d\lambda$$

In addition, based on the Marcus electron transfer theory [76, 77], the total reorganization energy could also affect the kinetics of electron injection, which can be approximately described as [78]:

$$K = A\exp(-\frac{\lambda}{4K_bT})$$

where A is a prefactor, λ is the total reorganization energies, k_b is the Boltzmann constant and T is the temperature. As a result, the enhancement of J_{sc} should focus on improving the λ.

3. RESULTS AND DISCUSSION

3.1. Electron injection investigation as sensitizers

We have tabulated the ΔG^{inject}, E_{OX}^{dye}, E_{OX}^{dye*}, λ_{max}^{ICT}, LHE, $|V_{RP}|$ and ΔG_r^{inject} in Table 1. Recently we have synthesized 2-{4-[2-(4-nitrobenzylidene)hydrazino)]phenyl}ethylene 1,1,2-tricarbonitrile (NBHPET) sensitizer [79]. The electron injection was calculated -0.39 and the electron coupling strength 0.195 [80]. In investigated derivatives, the $|V_{RP}|$ and ΔG_r^{inject} of naphtho[2,3-b]thiophene derivatives are superior as compared to the NBHPET. The basic structure of organic sensitizers is made of a donor (D), a bridge (B, π spacer), and an acceptor (A) moieties (D-π-A) to improve the efficiency. The donor moieties have been substituted at one end while acceptor units at opposite side which improved the ICT in newly designed sensitizers. Whilst in "NBHPET" the bridge is small as well as polarization increased from neutral to cation or anion species. Thus it is expected that naphtho[2,3-b]thiophene derivatives the electron injection is superior than "NBHPET".

Table 1. The ΔG^{inject}, oxidation potential, light harvesting efficiency (LHE), $|V_{RP}|$ of investigated dyes at TD-B3LYP/6-31G**//B3LYP/6-31G** level of theory.

System	ΔG^{inject}	E_{OX}^{dye}	E_{OX}^{dye*}	λ_{max}^{ICT}	*f*	*LHE*	ΔG^{inject}	$\|V_{RP}\|$
[a] NBHPET	-0.39	5.96	3.61	2.35	1.3189	0.9520	1.00	0.195
1	-2.05	5.47	1.95	3.52	0.3550	0.5584	5.26	1.025
	-1.36	5.47	2.64	2.83	0.2259	0.4056	3.49	0.680
	-1.00	5.47	3.00	2.47	0.1450	0.2838	2.56	0.500
2	-1.81	5.63	2.19	3.44	0.4480	0.6435	4.64	0.905
	-1.02	5.63	2.98	2.65	0.2269	0.4069	2.62	0.510
	-0.37	5.63	3.63	2.00	0.0592	0.1274	0.95	0.185
3	-2.25	5.25	1.75	3.50	0.5214	0.6990	5.77	1.125
	-1.17	5.25	2.42	2.83	0.2796	0.4747	3.00	0.585
	-1.07	5.25	2.93	2.32	0.1630	0.3129	2.74	0.535
4	-2.02	5.38	1.98	3.40	0.5290	0.7042	5.18	1.010
	-1.26	5.38	2.74	2.64	0.2507	0.4386	3.23	1.130
	-0.44	5.38	3.56	1.82	0.0678	0.1445	1.13	0.220
5	-2.21	5.31	1.79	3.52	0.4464	0.6422	5.67	1.105
	-1.52	5.31	2.48	2.83	0.2474	0.4343	3.90	0.760
	-1.04	5.31	2.96	2.35	0.1598	0.3078	2.67	1.020
6	-2.00	5.45	2.00	3.45	0.7033	0.8020	5.13	1.000
	-1.20	5.45	2.80	2.65	0.2202	0.3977	3.08	1.100
	-0.42	5.45	3.58	1.87	0.0664	0.1418	1.08	0.210

ΔG_r^{inject}= relative electron injection ΔG^{inject}(dye)/ ΔG^{inject}(NBHPET)

[a]Detail can be found in reference [80]

Three important excitations have been observed. The ΔG_r^{inject} for first, second and third transitions have been observed -1.00, -1.36 and -2.05, respectively for **1**. The $|V_{RP}|$ for first, second and third transitions have been observed 0.500, 0.680 and 1.025, respectively. In **2**, the ΔG_r^{inject} for first, second and third transitions have been observed -0.37, -1.02, and -1.81, respectively. The $|V_{RP}|$ for first, second and third transitions have been observed 0.185, 0.510, and 0.905, respectively. In **3**, the

ΔG_r^{inject} for first, second and third transitions have been observed -1.07, -1.17, and -2.25, respectively. The $|V_{RP}|$ for first, second and third transitions have been observed 0.535, 0.585, and 1.125, respectively. In **4**, the ΔG_r^{inject} for first, second and third transitions have been observed -0.44 -1.26, and -2.02, respectively. The $|V_{RP}|$ for first, second and third transitions have been observed 0.220, 0.630 and 1.010, respectively. In **5**, the ΔG_r^{inject} for first, second and third transitions have been observed -1.04 -1.52, and -2.21, respectively. The $|V_{RP}|$ for first, second and third transitions have been observed 0.520, 0.760 and 1.105, respectively. In **6**, the ΔG_r^{inject} for first, second and third transitions have been observed -0.42, -1.20, and -2.00, respectively. The $|V_{RP}|$ for first, second and third transitions have been observed 0.210, 0.600 and 1.000, respectively. The derivatives having COOH as substituent have higher ΔG_r^{inject} and $|V_{RP}|$ as compared to the derivatives containing NO_2. The strong electron activating group enhances ΔG_r^{inject} and $|V_{RP}|$. The azo dye based triaminopyrazolo[1,5-a]pyrimidine derivative (4b) showed ΔG_r^{inject} and $|V_{RP}|$ -1.19 and 0.53 at TD-B3LYP/6-31G*//B3LYP/6-31G* level of theory, respectively [81]. The ΔG_r^{inject} and $|V_{RP}|$ of hydrazone based sensitizer (system5) were found -0.61 and 0.305 at TD-B3LYP/6-31G*//B3LYP/6-31G* level of theory, respectively [80]. The ΔG_r^{inject} of 2TPA-R derivative of triphenylamine derivative for first and second excited states were observed -1.16 and -2.46 [82]. In present study, the ΔG_r^{inject} and $|V_{RP}|$ of new designed derivatives are revealing that these materials would be efficient visible light sensing/absorbing solar cell materials. The derivatives containing $–NO_2$ have superior LHE as compared to those systems which have –COOH. On the basis of electron activating groups the trend to enhance the LHE has been observed as $OCH_3 > OH > CH_3$.

3.2. Electronic properties investigation as hetero-junction solar cell materials

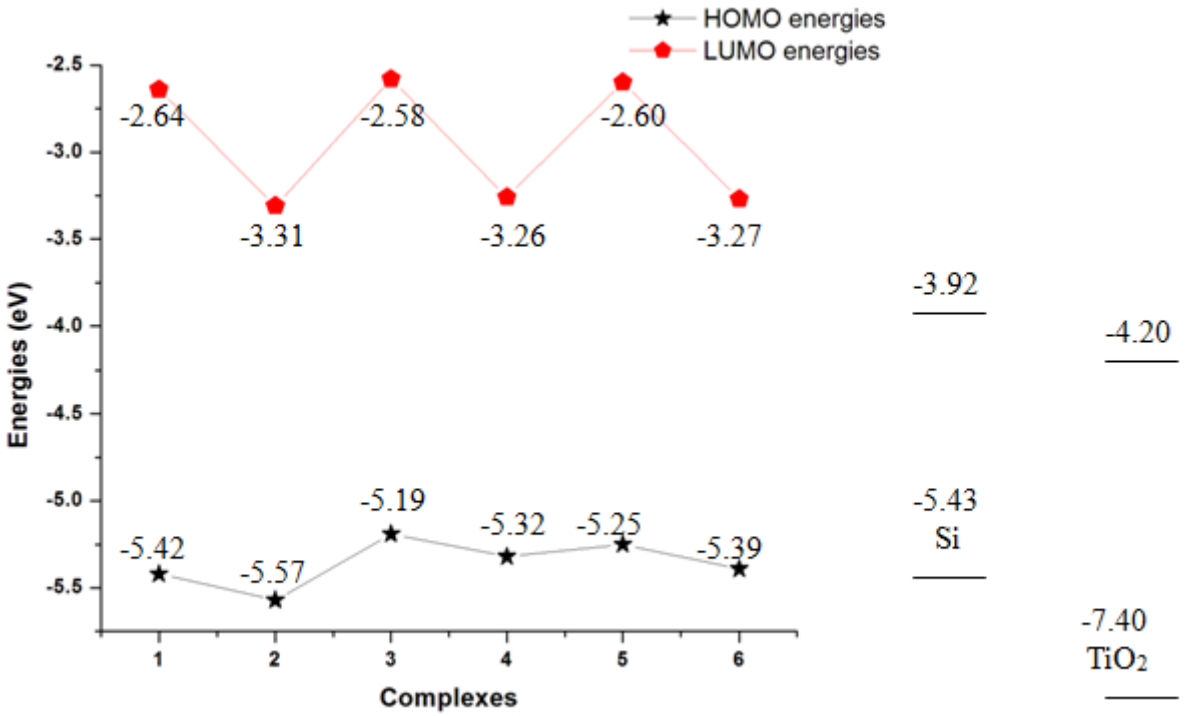

Figure 2. The HOMOs and LUMOs energies of donors and acceptors.

The HOMO and LUMO energies of Si are –5.43 and -3.92 eV, respectively [83]. The HOMO and LUMO energies of TiO_2 are –7.40 and -4.20 eV, respectively [84]. We have observed the Nested band alignment in the donor and acceptor frontier molecular orbitals by considering the Si as acceptor only. The successful operation of a photovoltaic device requires a staggered band alignment heterojunction which allocate electrons to transport to the cathode and holes to the anode. By considering the average values both for Si and TiO_2, the valance band energy has been found -6.41 eV while the conduction band energy -4.06 eV (Si/TiO_2). It is expected that Si/TiO_2 as acceptor changed the alignment to staggered band alignment heterojunction, see Fig. 2.

In hybrid solar cells, excitons formed in the donor material are dissociated at the D–A interface. The force required to overcome the exciton binding energy is provided by the energy level offset of the LUMO of the donor and the conduction band edge of the acceptor material [15]. We found energy level offset 1.42, 0.75, 1.48, 0.80, 1.46 and 0.79 eV for **1**-**6**, respectively to overcome the exciton binding energy. The nitro containing derivatives compared to –COOH bearing counterparts would be good materials for hetero-junction solar cells. For dissociation of excitons formed in the acceptor material, the energy offset of the HOMO of the donor and the valence band edge of the acceptor material is required. We found energy level offset 0.99, 0.84, 1.22, 1.09, 1.16 and 1.02 eV for **1**-**6**, respectively which showed that less energy would be required for nitro containing derivatives compared to –COOH bearing counterparts to dissociate of excitons. Scharber and coworkers concluded that V_{oc} is directly proportional to the diagonal band gap of the heterojunction [85].

The short circuit current density (J_{sc}) is directly related to the external quantum efficiency (EQE).

$$EQE = \eta_{abs} \times \eta_{diff} \times \eta_{diss} \times \eta_{tr} \times \eta_{cc}$$

The J_{sc} is directly linked with the absorption yield (η_{abs}). In this case, not only the inorganic part is improving the absorption yield but the organic materials are also covering most of the absorption spectra revealing it can absorb more solar spectrum region. The next important parameter is η_{diff} describes the ability of an exciton to diffuse to a D–A interface. This factor is inversely related to the rate of recombination within the photoactive material. The third parameter is the exciton dissociation yield (η_{diss}). As the electron is still bound within the exciton, the energy offset formed at the D–A interfaces is required to provide a driving force which releases the electron and allows conduction to occur [15]. This energy offset must be larger than the excitonic binding energy in the material to facilitate charge transfer. This energy is typically in the range of 0.1–0.5eV [86, 87]. In our case energy offset is larger than the excitonic binding energy revealing materials would be good charge transfer, see Fig. 2.

The fourth parameter describes the efficiency of charge carrier transport throughout the device (η_{tr}). In organic materials, charge transport occurs via a process of hopping between energy states and is affected by traps and recombination sites in the photoactive film [15]. The success of this transport depends greatly on the mobility of the associated semiconductors [88]. Moreover, the **2**, **4** and **6** have the high electron affinity which would improve the electron transport toward cathode.

The last important parameter describes the efficiency of charge collection at the electrodes (η_{cc}). The success of this step is greatly dependent on the electronic composition of the device. For

successful injection of electrons into the cathode, the magnitude of the conduction band edge energy level of the acceptor material, with respect to the vacuum level, must be lower than the work function of the metal. For successful injection of holes into the anode, the magnitude of the HOMO level of donor material must be higher than the work function of the transparent anode [15]. In our case HOMO energy levels of all studied sensitizers are higher than the anode [89].

Brabec et al. proposed an effective band gap model for bulk heterojunction cells; they correlated the maximum value of V_{oc} and the energy difference between the HOMO level of the donor and the LUMO level of the acceptor [90]. It is revealing that in our designed derivatives improved electron affinities of the donor materials would increase the V_{oc} ultimately efficiency. In the present study we observed the diagonal band gap of **1**-**6**, 1.36, 1.51, 1.13, 1.26, 1.19 and 1.33 eV, respectively. Moreover, these studies revealed that **2**, **4** and **6** would have superior V_{oc}. Previously it was pointed out that if the LUMO energy level of donor material would be less than -3.92 eV, it can improve the efficiency of organic solar cell devices [85]. In the present case the LUMO energies of **2**, **4** and **6** are smaller than other counterparts revealing these would be the efficient donors.

The poly (3-hexylthiophene) is being used as efficient donor material in solar cell devices due to the enhanced absorption, environmental stability and higher hole mobility [91]. The hole reorganization energies of naphthalene, anthracene, tetracene and pentacene at B3LYP/6-31G** level of theory are 0.186, 0.138, 0.114, 0.098 eV, respectively [89]. The hole reorganization energies of all studied derivatives except **4** are smaller than naphthalene. The smaller hole reorganization energies are revealing that these materials would be efficient hole transporters. The *mer*-Alq3 is efficient electron transfer material which has the electron reorganization energy 0.276 eV, the smaller or comparable electron reorganization energies of **1**-**3** and **5** are revealing that these materials would be efficient as electron transporters, see Table 2.

Table 2. The hole, electron reorganization energies and adiabatic electron affinities of studied systems at B3LYP/6-31G** level of theory.

Complexes	λ (h)	λ (e)	EA[a]
1	0.098	0.259	1.66
2	0.140	0.299	2.24
3	0.178	0.283	1.59
4	0.229	0.313	2.19
5	0.146	0.278	1.61
6	0.183	0.309	2.21

4. CONCLUSIONS

The electron injection and electron coupling constants of studied derivatives are superior as compared to the NBHPET. The derivatives having -COOH as substituent have higher electron injection and electron coupling constants than those derivatives having NO_2. The light harvesting efficiencies of **2**, **4** and **6** are higher than **1**, **3** and **5**. The higher electron injection and electron coupling constants revealed that all the studied dyes would be efficient dye-sensitized solar cell materials. The combination of Si/TiO_2 as acceptor materials might change the alignment to staggered band alignment heterojunction which is best for charge transfer from donors to acceptors. To overcome the exciton binding energy and dissociate of excitons less energy is required for **2**, **4** and **6** illuminating these would be efficient as hetero-junction hybrid solar cell materials. The higher electron affinities of **2**, **4** and **6** are enlightening that these would improve the electron transport toward cathode ultimately increase V_{oc}. The higher HOMO energy levels of all studied dyes than the anode resulting efficient hole transporters. The smaller or comparable hole and electron reorganization energies of **1-3** and **5** with referenced compounds enlightened that these would be efficient materials. The higher diagonal band gap for **2**, **4** and **6** showed that these dyes might have higher short-circuit current density (J_{sc}) and fill factor (FF) resulting improved solar cell efficiency.

ACKNOWLEDGEMENT
Authors would like to acknowledge the support of the Ministry of Higher Education, Kingdom of Saudi Arabia for this research through a Grant (PCSED-006-14) under the Promising Centre for Sensors and Electronic Devices (PCSED) at Najran University, Kingdom of Saudi Arabia.

References

1. J.P. Holdren, *Science*, 319 (2008) 424-434.
2. R.F. Service, *Science*, 309 (2005) 548-551.
3. E.A. Alsema, *Progress in Photovoltaics: Research and Applications*, 8 (2000) 17-25.
4. G. Li, K.-J. Jiang, Y.-F. Li, S.-L. Li, L.-M. Yang, *J. Phys. Chem*. C, 112 (2008) 11591-11599.
5. M.A. Green, K. Emery, Y. Hishikawa, W. Warta, E.D. Dunlop, *Progress in Photovoltaics: Research and Applications*, 20 (2012) 12-20.
6. G.P. Smestad, S. Spiekermann, J. Kowalik, C.D. Grant, A.M. Schwartzberg, J. Zhang, L.M. Tolbert, E. Moons, *Sol. Energy Mater. Sol. Cells*, 76 (2003) 85-105.
7. D. Gebeyehu, C.J. Brabec, N.S. Sariciftci, D. Vangeneugden, R. Kiebooms, D. Vanderzande, F. Kienberger, H. Schindler, *Synth. Met.*, 125 (2001) 279-287.
8. P.A. van Hal, M.M. Wienk, J.M. Kroon, W.J.H. Verhees, L.H. Slooff, W.J.H. van Gennip, P. Jonkheijm, R.A.J. Janssen, *Adv. Mater*., 15 (2003) 118-121.
9. W.J.E. Beek, M.M. Wienk, R.A.J. Janssen, *Adv. Funct. Mater*., 16 (2006) 1112-1116.
10. A.P. Alivisatos, *Science*, 271 (1996) 933-937.
11. W.U. Huynh, J.J. Dittmer, A.P. Alivisatos, *Science*, 295 (2002) 2425-2427.
12. N.C. Greenham, X. Peng, A.P. Alivisatos, *Phys. Rev*. B, 54 (1996) 17628-17637.
13. S.A. McDonald, G. Konstantatos, S. Zhang, P.W. Cyr, E.J.D. Klem, L. Levina, E.H. Sargent, *Nat Mater*, 4 (2005) 138-142.
14. E. Arici, N.S. Sariciftci, D. Meissner, *Adv. Funct. Mater*., 13 (2003) 165-171.
15. M. Wright, A. Uddin, *Sol. Energy Mater. Sol. Cells*, 107 (2012) 87-111.

16. J.-S. Huang, C.-Y. Hsiao, S.-J. Syu, J.-J. Chao, C.-F. Lin, *Sol. Energy Mater. Sol. Cells*, 93 (2009) 621-624.
17. H.-J. Syu, S.-C. Shiu, C.-F. Lin, *Sol. Energy Mater. Sol. Cells*, 98 (2012) 267-272.
18. S.-H. Tsai, H.-C. Chang, H.-H. Wang, S.-Y. Chen, C.-A. Lin, S.-A. Chen, Y.-L. Chueh, J.-H. He, *ACS Nano*, 5 (2011) 9501-9510.
19. L. He, C. Jiang, Rusli, D. Lai, H. Wang, *Appl. Phys. Lett.*, 99 (2011) 021104-021103.
20. C.-Y. Liu, Z.C. Holman, U.R. Kortshagen, *Adv. Funct. Mater.*, 20 (2010) 2157-2164.
21. Y. Zhou, M. Eck, M. Kruger, *Energy Environ. Sci.*, 3 (2010) 1851-1864.
22. T. Xu, Q. Qiao, *Energy Environ. Sci.*, 4 (2011) 2700-2720.
23. M. Wiemer, V. Sabnis, H. Yuen, 43.5% efficient lattice matched solar cells, in, 2011, pp. 810804-810804-810805.
24. S. Ernst, W. Kaim, *J. Am. Chem. Soc.*, 108 (1986) 3578-3586.
25. G. Hughes, M.R. Bryce, *J. Mater. Chem.*, 15 (2005) 94-107.
26. K. Van De Wetering, C. Brochon, C. Ngov, G. Hadziioannou, *Macromolecules*, 39 (2006) 4289-4297.
27. W. Wu, Y. Liu, D. Zhu, *Chem. Soc. Rev.*, 39 (2010) 1489-1502.
28. C. Goldmann, S. Haas, C. Krellner, K.P. Pernstich, D.J. Gundlach, B. Batlogg, *J. Appl. Phys.*, 96 (2004) 2080-2086.
29. A. IRFAN, A.G. AL-SEHEMI, *J. Chem. Soc. Pak.*, 34 (2012) 350.
30. A. Irfan, A.G. Al-Sehemi, A.M. Asiri, M. Nadeem, K.A. Alamry, *Comp. Theor. Chem*, 977 (2011) 9-12.
31. A. Irfan, *Comp. Mater. Sci.*, 81 (2014) 488-492.
32. A. Irfan, A.G. Al-Sehemi, M.S. Al-Assiri, *J. Fluorine Chem.*, 157 (2014) 52-57.
33. A. Irfan, A.G. Al-Sehemi, M.S. Al-Assiri, *Comp. Theor. Chem*, 1031 (2014) 76-82.
34. A. Irfan, A.G. Al-Sehemi, S. Muhammad, *Synth. Met.*, 190 (2014) 27-33.
35. A.G. Al-Sehemi, A. Irfan, M.A.M. Al-Melfi, A.A. Al-Ghamdi, E. Shalaan, *J. Photochem. Photobiol., A: Chem.*, 292 (2014) 1-9.
36. A.R. Chaudhry, R. Ahmed, A. Irfan, A. Shaari, A.G. Al-Sehemi, *Science of Advanced Materials*, 6 (2014) 1727-1739.
37. A.R. Chaudhry, R. Ahmed, A. Irfan, S. Muhammad, A. Shaari, A.G. Al-Sehemi, *Comp. Theor. Chem*, 1045 (2014) 123-134.
38. A.G. Al-Sehemi, A. Irfan, A.M. Asiri, *Chin. Chem. Lett.*, 25 (2014) 609-612.
39. A. Irfan, *J. Theor. Comput. Chem.*, 13 (2014) 1450013.
40. A.R. Chaudhry, R. Ahmed, A. Irfan, A. Shaari, H. Maarof, A.G. Al-Sehemi, *Sains Malaysiana*, 43 (2014) 867-875.
41. A. Irfan, A.G. Al-Sehemi, S. Muhammad, *Journal of Quantum Chemistry*, 2014 (2014) 6.
42. A. Irfan, *Optik - Intern. J. Light Elect. Optics*, 125 (2014) 4825-4830.
43. A. Irfan, A.G. Al-Sehemi, S. Muhammad, J. Zhang, *Australian Journal of Chemistry*, 64 (2011) 1587-1592.
44. A. Irfan, R. Jin, A.G. Al-Sehemi, A.M. Asiri, *Spectrochimica Acta Part A: Molecular and Biomolecular Spectroscopy*, 110 (2013) 60-66.
45. A.I.A. Mahmood, *Journal of Computational Electronics*, (2013).
46. A. Irfan, F. Ijaz, A.G. Al-Sehemi, A.M. Asiri, *Journal of Computational Electronics*, (2012) 1-11.
47. A. Irfan, R. Cui, J. Zhang, *Chem. Phys.*, 358 (2009) 25-29.
48. A. Irfan, J. Zhang, *Theoretical Chemistry Accounts*, 124 (2009) 339-344.
49. A. Irfan, R. Cui, J. Zhang, *Theoretical Chemistry Accounts*, 122 (2009) 275-281.
50. A. Irfan, R. Cui, J. Zhang, *J. Mol. Struct.* (TheoChem), 956 (2010) 61-65.
51. A. Irfan, J. Zhang, Y. Chang, *Theoretical Chemistry Accounts*, 127 (2010) 587-594.
52. M. J. Frisch et al., Inc., Wallingford, CT, (2009).
53. A.D. Becke, *J. Chem. Phys.*, 98 (1993) 5648-5652.

54. B. Miehlich, A. Savin, H. Stoll, H. Preuss, *Chem. Phys. Lett.*, 157 (1989) 200-206.
55. C. Lee, W. Yang, R.G. Parr, *Phys. Rev.* B, 37 (1988) 785-789.
56. W. Xu, B. Peng, J. Chen, M. Liang, F. Cai, *J. Phys. Chem.* C, 112 (2008) 874-880.
57. J. Sun, J. Song, Y. Zhao, W.-Z. Liang, *J. Chem. Phys*., 127 (2007) 234107-234107.
58. C. Zhang, W. Liang, H. Chen, Y. Chen, Z. Wei, Y. Wu, *J. Mol. Struct*. (TheoChem), 862 (2008) 98-104.
59. D. Matthews, P. Infelta, M. Grätzel, *Sol. Energy Mater. Sol. Cells*, 44 (1996) 119-155.
60. G. Pourtois, D. Beljonne, J. Cornil, M.A. Ratner, J.L. Brédas, *J. Am. Chem. Soc*., 124 (2002) 4436-4447.
61. C.-P. Hsu, *Acc. Chem. Res*., 42 (2009) 509-518.
62. R.A. Marcus, *Reviews of Modern Physics*, 65 (1993) 599-610.
63. M. Hilgendorff, V. Sundström, *J. Phys. Chem*. B, 102 (1998) 10505-10514.
64. J. Asbury, Y.-Q. Wang, E. Hao, H. Ghosh, T. Lian, *Res. Chem. Intermed.*, 27 (2001) 393-406.
65. R. Katoh, A. Furube, T. Yoshihara, K. Hara, G. Fujihashi, S. Takano, S. Murata, H. Arakawa, M. Tachiya, *J. Phys. Chem*. B, 108 (2004) 4818-4822.
66. A. Hagfeldt, M. Graetzel, *Chem. Rev.*, 95 (1995) 49-68.
67. P.F. Barbara, T.J. Meyer, M.A. Ratner, *J. Phys. Chem.*, 100 (1996) 13148-13168.
68. S.F.a.A.S. Filippo De Angelis, *Nanotechnology* 19 (2008) 424002-424008.
69. G. Benkö, J. Kallioinen, J.E.I. Korppi-Tommola, A.P. Yartsev, V. Sundström, *J. Am. Chem. Soc.*, 124 (2001) 489-493.
70. S. Iwai, K. Hara, S. Murata, R. Katoh, H. Sugihara, H. Arakawa, *J. Chem. Phys*., 113 (2000) 3366-3373.
71. J. Preat, C. Michaux, D. Jacquemin, E.A. Perpète, *J. Phys. Chem*. C, 113 (2009) 16821-16833.
72. H.S. Nalwa, in, Handbook of advanced electronic and photonic materials and devices, Academic: San Diego CA, 2001.
73. M. Cassida, in, recent Advances in density Functional Methods: Time dependent density functional response Theory for molecules, DP Chong: Singapore, 1995.
74. M.D.B. D.C. Harris, in, Symmetry and Spectroscopy, Dover: New York US, 1998.
75. J. Zhang, Y.-H. Kan, H.-B. Li, Y. Geng, Y. Wu, Y.-A. Duan, Z.-M. Su, *J. Mol. Model*., 19 (2013) 1597-1604.
76. R.A. Marcus, *J. Chem. Phys.*, 43 (1965) 679-701.
77. N.A. Anderson, T. Lian, *Annu. Rev. Phys. Chem*., 56 (2004) 491-519.
78. M.P. Balanay, D.H. Kim, *J. Mol. Struct.* (TheoChem), 910 (2009) 20-26.
79. A.G. Al-Sehemi, A. Irfan, A.M. Asiri, Y.A. Ammar, *J. Mol. Struct*., 1019 (2012) 130-134.
80. A. Al-Sehemi, A. Irfan, A. Asiri, *Theoretical Chemistry Accounts*, 131 (2012) 1-10.
81. A.G. Al-Sehemi, A. Irfan, A.M. Fouda, *Spectrochimica Acta Part A: Molecular and Biomolecular Spectroscopy*, 111 (2013) 223-229.
82. J. Preat, *J. Phys. Chem*. C, 114 (2010) 16716-16725.
83. C.-Y. Liu, Z.C. Holman, U.R. Kortshagen, *Nano Lett.*, 9 (2008) 449-452.
84. C.Y. Kuo, W.C. Tang, C. Gau, T.F. Guo, D.Z. Jeng, *Appl. Phys. Lett*., 93 (2008) 033307-033303.
85. M.C. Scharber, D. Mühlbacher, M. Koppe, P. Denk, C. Waldauf, A.J. Heeger, C.J. Brabec, *Adv. Mater.*, 18 (2006) 789-794.
86. C.J. Brabec, S. Gowrisanker, J.J.M. Halls, D. Laird, S. Jia, S.P. Williams, *Adv. Mater.*, 22 (2010) 3839-3856.
87. B.A. Gregg, M.C. Hanna, *J. Appl. Phys*., 93 (2003) 3605-3614.
88. V.D. Mihailetchi, H.X. Xie, B. de Boer, L.J.A. Koster, P.W.M. Blom, *Adv. Funct. Mater.*, 16 (2006) 699-708.
89. A. Irfan, A.G. Al-Sehemi, M.S. Al-Assiri, *J. Mol. Graphics Modell.*, 44 (2013) 168-176.
90. C.J. Brabec, A. Cravino, D. Meissner, N.S. Sariciftci, T. Fromherz, M.T. Rispens, L. Sanchez, J.C. Hummelen, *Adv. Funct. Mater*., 11 (2001) 374-380.

91. [X. Yang, J. Loos, S.C. Veenstra, W.J.H. Verhees, M.M. Wienk, J.M. Kroon, M.A.J. Michels, R.A.J. Janssen, *Nano Lett*., 5 (2005) 579-583.